NASA TECHNICAL NOTE

NASA TN D-5187

C. 1

NASA TN D-5187

EXPLORER XXXV ATTITUDE CONTROL SYSTEM

by J. V. Fedor, T. W. Flatley, M. F. Federline,
and J. R. Metzger

Goddard Space Flight Center
Greenbelt, Md.

EXPLORER XXXV ATTITUDE CONTROL SYSTEM

By J. V. Fedor, T. W. Flatley,
M. F. Federline, and J. R. Metzger

Goddard Space Flight Center
Greenbelt, Md.

NATIONAL AERONAUTICS AND SPACE ADMINISTRATION

ABSTRACT

This report deals with background history, system description, system operation, maneuvering concept and theory, gas bearing testing, and preliminary flight performance of the attitude control system used on the AIMP E spacecraft (Explorer XXXV), launched July 19, 1967.

CONTENTS

EXPLORER XXXV ATTITUDE CONTROL SYSTEM

by
J. V. Fedor, T. W. Flatley,
M. F. Federline, and J. R. Metzger
Goddard Space Flight Center

INTRODUCTION

In mid-1965, it was tentatively decided to include an active attitude control system (ACS) on IMP H and J (future spacecraft in the Interplanetary Monitoring Probe series) to put the spin axis of the spacecraft perpendicular to the sun's rays in a closed loop fashion. This maneuver would eliminate the need for separate solar paddles by improving the overall output of solar cells on the spacecraft, permit more space and weight for the payload, and simplify the thermal design. Since certain components of the system were new technology, it was decided that as much of the ACS as possible would be flown on an early launch (AIMP E) as a development experiment to flight-qualify the system. With these guidelines, a closed loop automatic system was designed.

During the latter part of June 1966, AIMP D was launched and did not achieve a desired lunar orbit. Postflight analysis indicated that if the spacecraft spin axis had been moved 10 degrees during the transfer trajectory and before last stage (retro) burn, a lunar orbit would have been achieved. With this added motivation, the status of the ACS was changed from a development experiment to an in-line flight system. The control system was modified so that it could precess the spin axis in four orthogonal directions (toward the sun and away from the sun and perpendicular to this) and so point the spin axis of the spacecraft in any arbitrary direction for retromotor burn. AIMP E was launched in July 1967, and was designated Explorer XXXV. The attitude control system made two flawless orientation maneuvers: One attitude correction of 5.55 degrees prior to retromotor firing and lunar orbit capture, and later a 120-degree change of orientation to put the spin axis perpendicular to the ecliptic plane. Further, the AIMP E spacecraft was the first flight of a simplified electronic four-quadrant spin-attitude control system.

ATTITUDE CONTROL SYSTEM DESCRIPTION

The ACS evolved is simple and light in weight, ideally suited for small scientific satellites. The basic components of the control system are control logic electronics for direction and thruster pulse width operation, thrusters for torquing, and a nutation damper. The spatial arrangement of the components on Explorer XXXV is shown in Figure 1. Operationally, the components mentioned above are tied into the telemetry and command, sun aspect sensor, and attitude determination
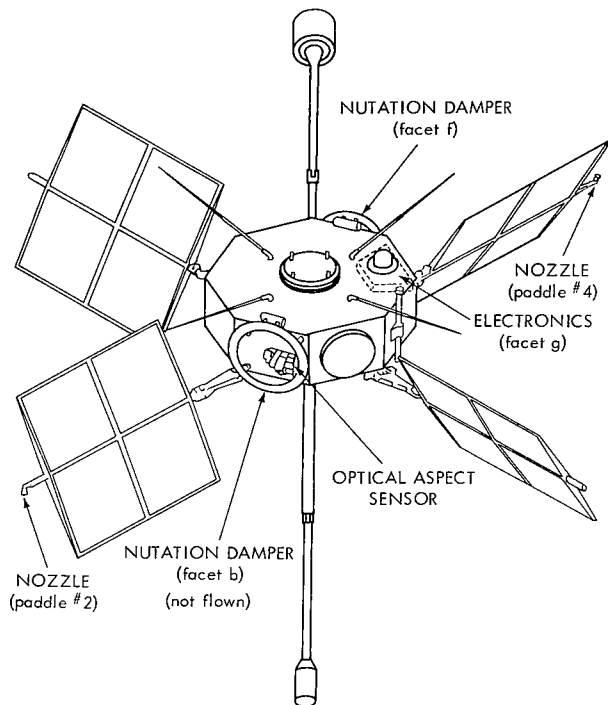
Figure 1—Spatial arrangement of ACS components on Explorer XXXV.

systems. Since these latter items are normally flown on a spacecraft, the ACS can be added or deleted as required by the program mission.

An ACS operation block diagram is shown in Figure 2. Basically, the system functions as follows: Assuming it is desired to move the spin axis in a given direction (toward the sun, away from the sun, or around the satellite-sun line), a direction command is sent from the ground station. This command is stored in a register in the control logic. Upon verification of the direction command, an execute command will cause the control logic to deliver pulses to the solenoids of the thrusters, one pulse per spin period, an action which precesses the spin axis in the desired direction. After a fixed time (2.74 minutes for Explorer XXXV), a pulse from the spacecraft clock stops the operation of the electronics and hence the thrusters. The nutation damper eliminates any residual nutation angle in a short time, and spacecraft attitude information can be relayed to the ground station to assess the inertial orientation of the spin axis. This is open-loop spacecraft precession with the maneuvering loop closed on the ground. The above sequence can be repeated as often as needed to achieve a certain attitude in space.
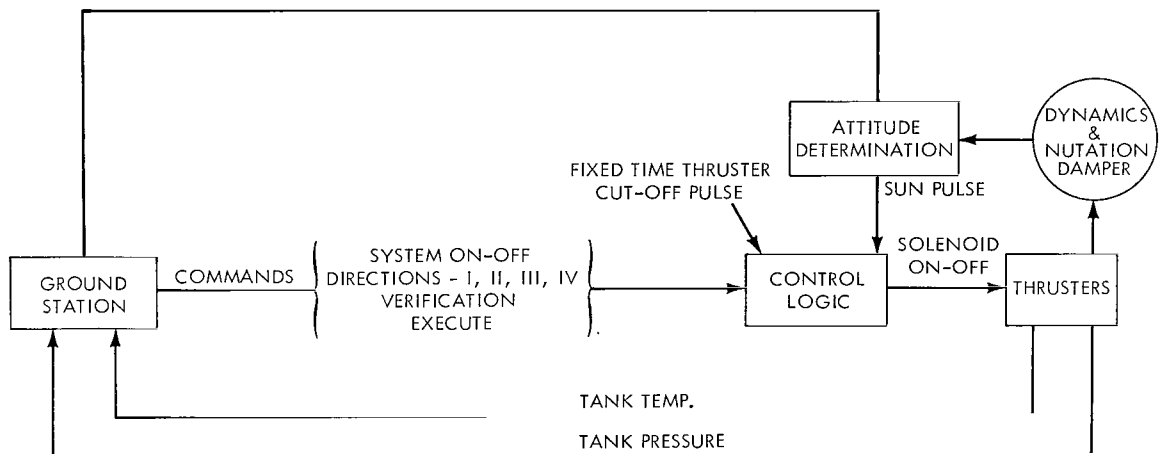

Figure 2—Explorer XXXV attitude control system, operation block diagram.

DESCRIPTION OF COMPONENTS

The following is a brief description of the control logic electronics, the thrusters, and the nutation damper.

Control Logic Electronics

The control logic electronics in the ACS is somewhat different from any previously used. It is based upon the concept of digitally processing sun aspect sensor information for quadrant direction and solenoid pulse width. The function of the control logic electronics is to generate, upon command, a series of solenoid drive pulses at 0, 90, 180, or 270 degrees of rotation following an optical aspect sun pulse. It is further required that the solenoid drive pulse width be 1/16 of a revolution. This is achieved in the following way (see Figure 3): The period of the sun pulses is measured, divided by 16 and stored digitally as a reference. From this reference, 16 pulses are then generated during one sun pulse period. It is the periods of these 16 pulses that determine the solenoid drive pulse width. The 16 pulses are then divided by 4 to obtain the quadrant pulses (0,
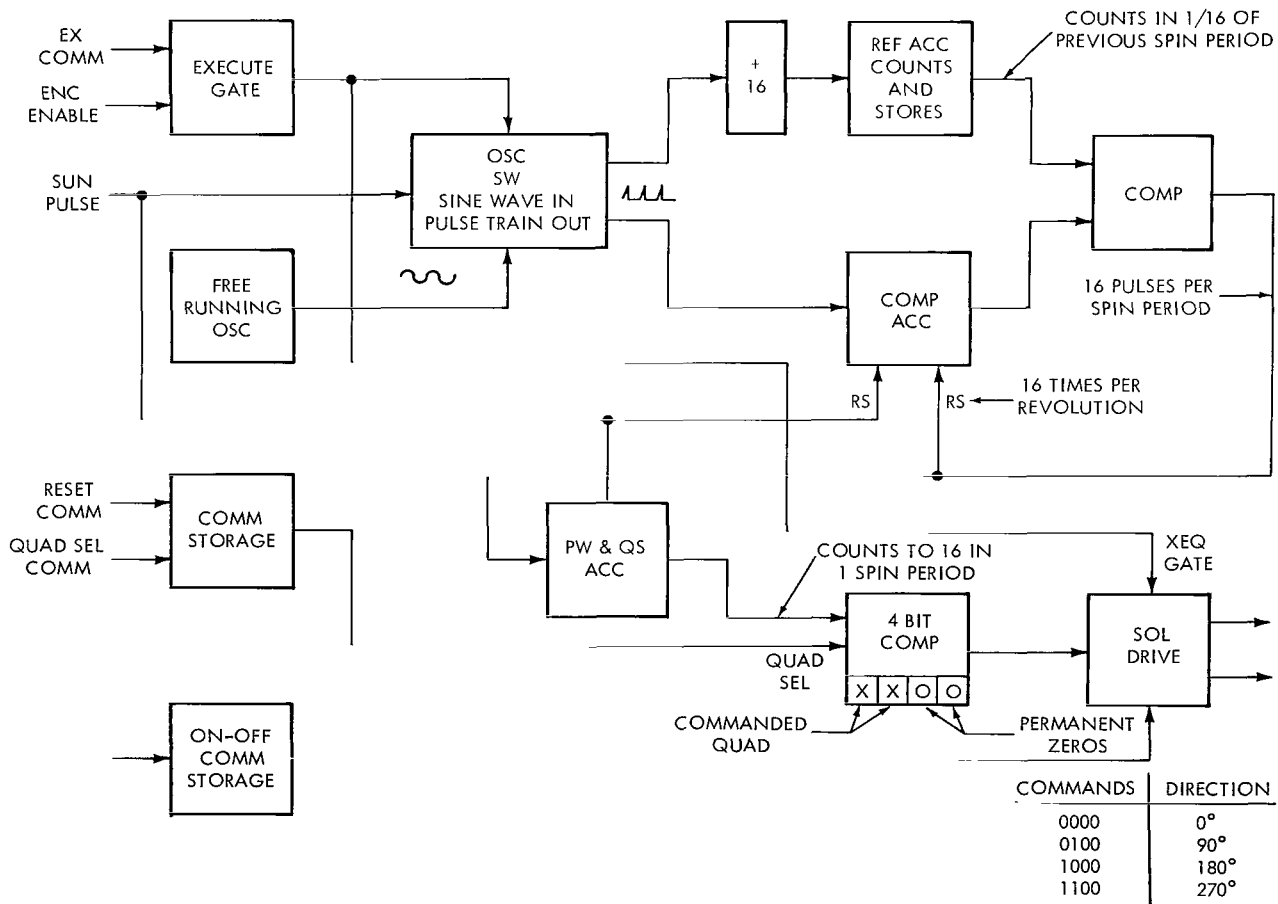
Figure 3—Explorer XXXV attitude control electronics.

COMMANDS	DIRECTION
0000	0°
0100	90°
1000	180°
1100	270°

90, 180, or 270 degrees). The quadrant pulses are compared to a command storage register which has a code representing 0, 90, 180, or 270 degrees. At coincidence of the codes a solenoid drive pulse is generated. Solenoid drive pulses are generated for a fixed duration (2.7 minutes, a convenient time interval for Explorer XXXV), at the end of which time a stop pulse is delivered by the spacecraft master clock.

A schematic diagram of the sun aspect sensor used on Explorer XXXV is shown in Figure 4. The sensor consists of a quartz window, gray code mask, solar cells, and amplifiers. This unit is commercially available. Two units are used back-to-back to achieve 180° aspect sensing.

Thrusters

Subliming solid thrusters, a new technology, were initially considered for the ACS. Technical problems as well as the flight program schedule prevented the installation of the subliming solid thrusters on Explorer XXXV. Appendix A describes the subliming thrusters and some of the problems encountered during the flight program. A conventional "Freon 14" thruster system was eventually used for the flight system. This system was designed to fit on the spacecraft in the same way as the subliming system. A block diagram of the Freon thrusters is shown in Figure 5. Redundancy and reliability are obtained by having two thrusters (only one is absolutely necessary), and two valves in series per thruster. Nominal steady-state thruster level is .016 lb, and distance between nozzles is 8.3 feet.

Nutation Damper

The ACS nutation damper is of the fluid-in-a-ring type. A unit is mounted on one of the facets of the spacecraft cover (see Figure 1). The damper is 1-inch diameter aluminum tubing formed into a ring of 10.75-inch mean diameter. The fluid used is Dow Corning #200 Silicone Oil. The adjustable viscosity allows the damper to be "tuned" so that the energy dissipation can be at the
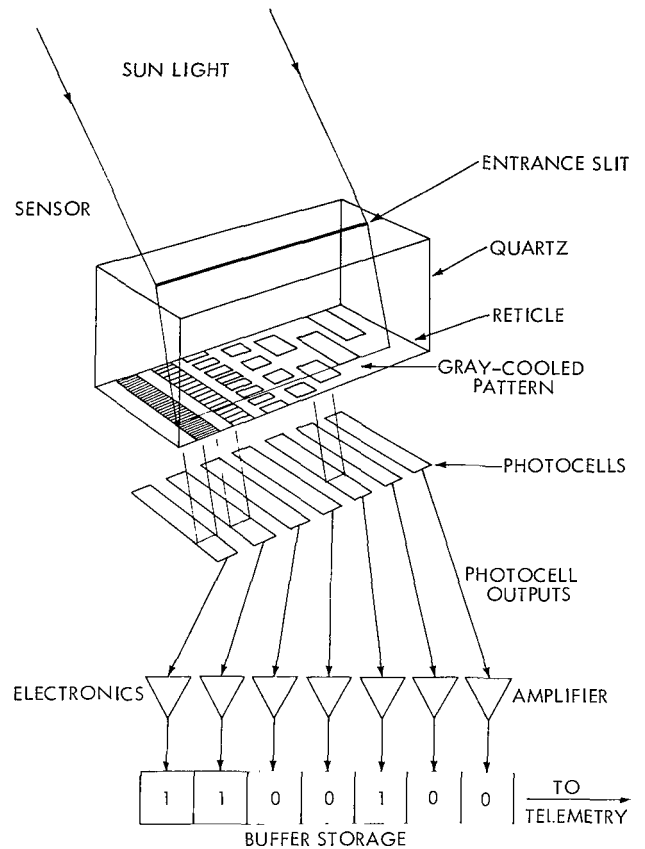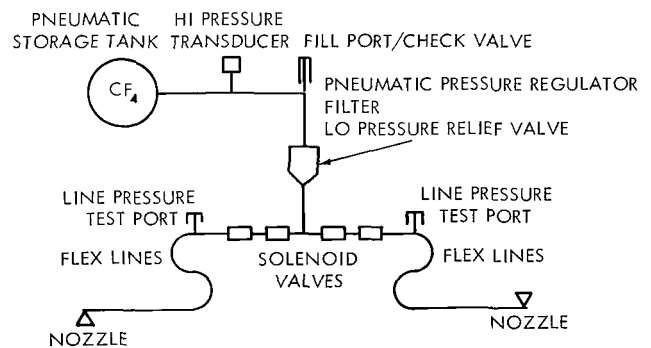

Figure 4—Functional diagram of sun aspect sensor.

Figure 5—Freon thruster system schematic.

maximum. A 2-inch reservoir is located on the inboard side for temperature expansion of the fluid. During flight, centrifugal force tends to keep the main ring filled with fluid. A fill port arrangement in the reservoir allows for leak checking, evacuating for filling, and sealing prior to disconnection from the fluid supply. The damper weighs approximately 1.27 lb, which includes 390 grams (.861 lb) of fluid. The unit produces a time constant of about 20 minutes during the mission phase. Appendix B gives design details of the damper. Time constant information is for two dampers; only one was flown, because of a last-minute weight problem.

SPIN-AXIS PRECESSION CONCEPT AND GEOMETRY

Conceptually, the ACS provides a torque on the spacecraft which is perpendicular to the spin axis and in one of four directions relative to the plane defined by the spin axis and the spacecraft-sun line as shown in Figure 6. Table 1 shows the various possible torques in vector form. The motion of the system is governed by

$$\frac{d}{dt} \vec{H} = \vec{T}$$

where

$\vec{H}$ = angular momentum, and

$\vec{T}$ = torque.

In the analysis that follows, only the gross torqued dynamic motion is considered and none of the fine structured torque-free motion. As long as the spin to transverse inertia ratio is not 1 or 2, the fine detailed motion is not significant.

$\vec{k}$ = UNIT VECTOR ALONG SPIN AXIS

$\vec{s}$ = UNIT VECTOR TOWARD SUN

θ = SUN ASPECT ANGLE

NOTE: IN GENERAL, $\vec{T} \cdot \vec{k} = 0$
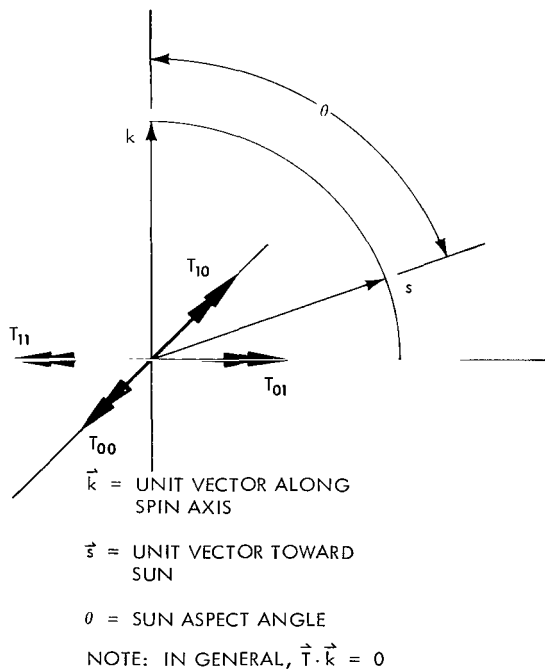
Figure 6—Possible control torque.

Table 1

Torques in Vector Form.

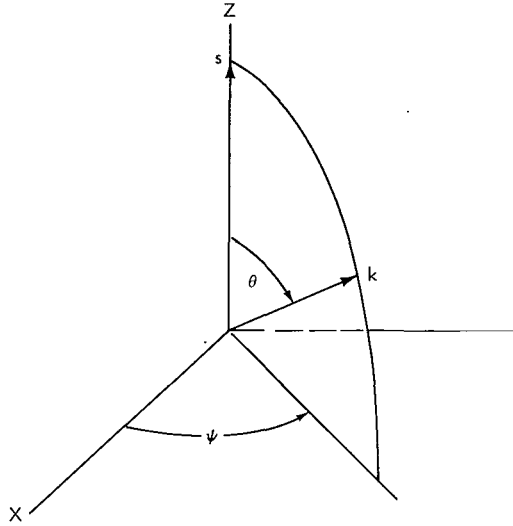| Mode	Torque
00	$\vec{T}_{00} = \dfrac{T}{\sin \theta} \, \vec{s} \times \vec{k}$
01	$\vec{T}_{01} = \dfrac{T}{\sin \theta} \, \vec{k} \times (\vec{s} \times \vec{k})$
10	$\vec{T}_{10} = \dfrac{T}{\sin \theta} \, \vec{k} \times \vec{s}$
11	$\vec{T}_{11} = \dfrac{T}{\sin \theta} \, \vec{k} \times (\vec{k} \times \vec{s})$

Figure 7—Inertial coordinate system.

If we assume $\vec{H} = H\vec{k}$—that is, the momentum is along the spin axis—then $\vec{H} \cdot \vec{T} = 0$ and it follows that $H = $ constant, and the motion of the spin axis is governed by

$$\frac{d}{dt} \vec{k} = \frac{\vec{T}}{H} .$$

Now consider an inertial coordinate system with one axis aligned with $\vec{s}$, and locate $\vec{k}$ by an angle θ with respect to $\vec{s}$ and an angle ψ with respect to an arbitrary axis normal to $\vec{s}$ as shown in Figure 7.

For mode 00 we have

$$\frac{d}{dt} \vec{k} = \frac{T}{H \sin \theta} \vec{s} \times \vec{k} .$$

Dotting both sides by $\vec{s}$,

$$\vec{s} \cdot \frac{d}{dt} (\vec{k}) = \frac{T}{H \sin \theta} \vec{s} \times \vec{k} \cdot \vec{s} = 0 ,$$

or

$$\vec{k} \cdot \vec{s} = \cos \theta = \text{constant} ,$$

since $\vec{s}$ is a constant vector.

Thus $\vec{k}$ merely rotates around $\vec{s}$ with a precession rate

$$\vec{\omega}_p = \dot{\psi} \vec{s} ,$$

and we can write

$$\frac{d}{dt} \vec{k} = \vec{\omega}_p \times \vec{k} .$$

Combining equations,

$$\dot{\psi} \vec{s} \times \vec{k} = \frac{T}{H \sin \theta} \vec{s} \times \vec{k} ,$$

6

hence

$$\dot{\psi}_{00} = \frac{T}{H \sin \theta} \cdot$$

In mode 01, the torque is "in plane" with respect to $\vec{k}$ and $\vec{s}$, so the spin axis will move toward or away from the sun line. Then ψ = constant, and

$$\vec{\omega}_p = \dot{\theta} \frac{\vec{s} \times \vec{k}}{\sin \theta} \cdot$$

Again combining equations,

$$\dot{\theta} \frac{(\vec{s} \times \vec{k})}{(\sin \theta)} \times \vec{k} = \frac{T}{H \sin \theta} \vec{k} \times (\vec{s} \times \vec{k}) ,$$

$$\dot{\theta}_{01} = -\frac{T}{H} \cdot$$

Similar developments can show that

$$\dot{\psi}_{10} = -\frac{T}{H \sin \theta} ,$$

$$\dot{\theta}_{11} = \frac{T}{H} \cdot$$
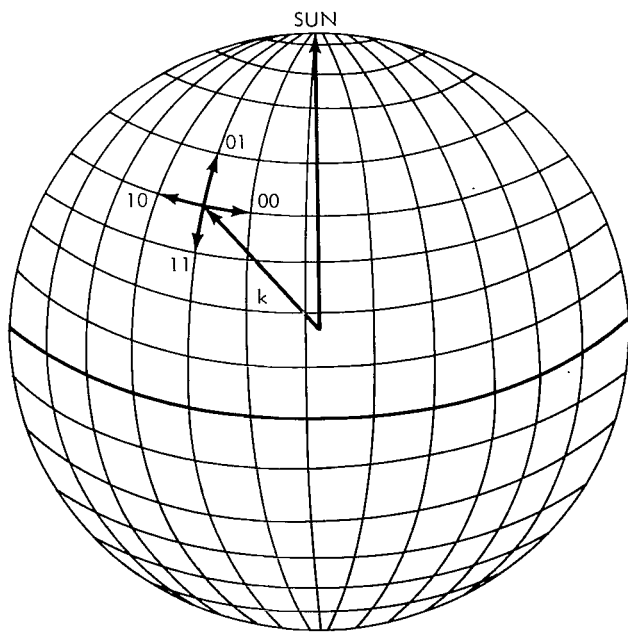
Figure 8—"Geographic" coordinate system.

If we think of $\vec{s}$ as locating the north pole of "geographic" coordinates, θ becomes a co-latitude and ψ a longitude (Figure 8), and the operation of the ACS can be summarized as in Table 2.

Table 2

Operational Torque Mode Summary.

Mode	Direction	Rate
00	East	$\dfrac{T}{H \sin \theta}$
01	North	$\dfrac{T}{H}$
10	West	$\dfrac{T}{H \sin \theta}$
11	South	$\dfrac{T}{H}$

A comment should be made about the theoretical precession rates given in Table 2. The preceding analysis is based on a steady applied torque. Since there is one torque pulse per rotation period, the precession rates should be multiplied by the fraction of a rotation period that the thrusters are on and a pulse efficiency factor. For Explorer XXXV, because of the short pulse width, the efficiency factor is essentially one, and the pulse period fraction is 1/16.

GAS BEARING FACILITY FOR SYSTEM TESTING

A significant contributing factor in the success of the ACS on Explorer XXXV was a gas bearing and ground station facility, developed at the Goddard Space Flight Center which permitted testing of the attitude control system. Some of the significant capabilities of the gas bearing are as follows:

1. Remote spinup and caging while spinning.

2. Remote dynamic balancing and compensation for unbalance caused by thruster fuel consumption.

3. Remote recharging of dc power supply without opening the vacuum chamber.

4. Ability to precess the gas bearing platform ±45 degrees from the local vertical.

5. Real-time display of spin axis position in space with 0.1° accuracy. During maneuvers, spin axis orientation can be determined to within 0.01° by the attitude determination system.

6. Bearing platform telemetry with capability of transmitting all significant ACS parameters to a ground station.

Figure 9 shows a conceptual schematic of the test setup; Figure 10 shows the gas bearing in a vacuum chamber with the attitude control system on the satellite simulator. This simulator, rotating on a spherical gas bearing, had moments of inertia closely matching those of the satellite. In addition to the fuel tank and thruster system, it carried batteries for power, a command receiver and data transmitter, and nutation dampers; and was equipped for remote battery charging, balancing, and spin control.

On the spacecraft, the sun aspect sensor, attitude control electronics, and solenoid drivers are all hard-line-connected. During dynamic testing, certain operational details were changed in order to avoid the need for a sun sensor and solar simulation, and to make the control electronics accessible from outside the chamber. A lamp was placed on the simulator in a position corresponding to the sun sensor location on the spacecraft. A "see sun" signal, generated when the lamp illuminated one of two attitude determination arrays, was fed directly into the control electronics. The solenoid drive signal was then telemetered to the simulator. Electronic delays, due chiefly to the receiver response, were measured and compensated for during data reduction.

The attitude determination arrays each consisted of a string of solar cells in a vertical plane and lying on a circular arc struck from the center of the gas bearing. The width of each cell corresponded to 1/8 of one degree of arc. The cells were illuminated by a beam of light perpendicular
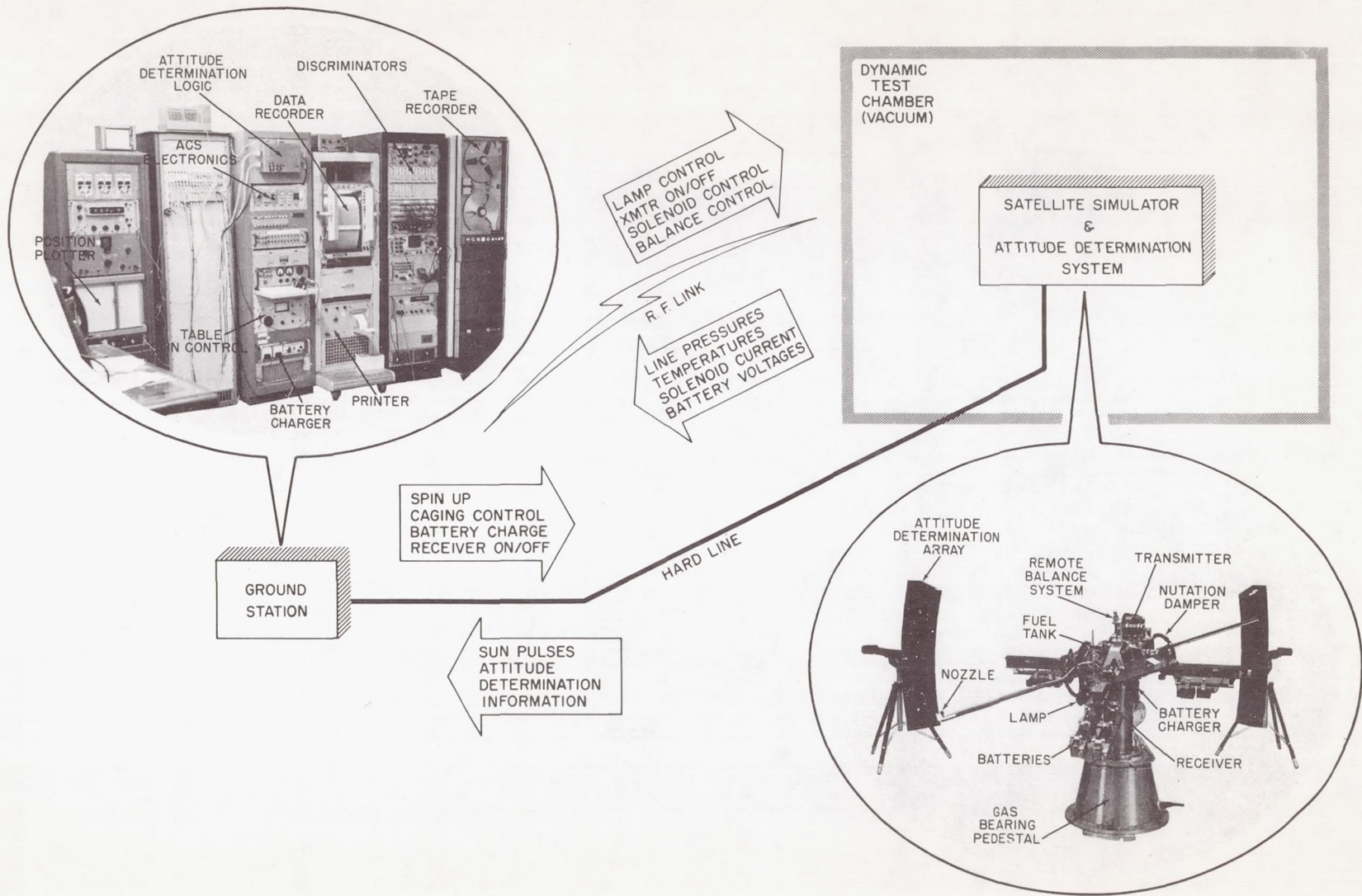
8

Figure 9—ACS simulation schematic.

Labels in the figure:

Upper left oval (ground equipment):
- ATTITUDE DETERMINATION LOGIC
- DISCRIMINATORS
- DATA RECORDER
- TAPE RECORDER
- ACS ELECTRONICS
- POSITION PLOTTER
- TABLE SPIN CONTROL
- BATTERY CHARGER
- PRINTER

Upper right box:
- DYNAMIC TEST CHAMBER (VACUUM)
- SATELLITE SIMULATOR & ATTITUDE DETERMINATION SYSTEM

Arrows:
- LAMP CONTROL / XMTR ON/OFF / SOLENOID CONTROL / BALANCE CONTROL
- R.F. LINK
- LINE PRESSURES / TEMPERATURES / SOLENOID CURRENT / BATTERY VOLTAGES
- SPIN UP / CAGING CONTROL / BATTERY CHARGE / RECEIVER ON/OFF
- HARD LINE
- SUN PULSES / ATTITUDE DETERMINATION INFORMATION

Center:
- GROUND STATION

Lower right oval (satellite):
- ATTITUDE DETERMINATION ARRAY
- REMOTE BALANCE SYSTEM
- TRANSMITTER
- NUTATION DAMPER
- FUEL TANK
- NOZZLE
- LAMP
- BATTERY CHARGER
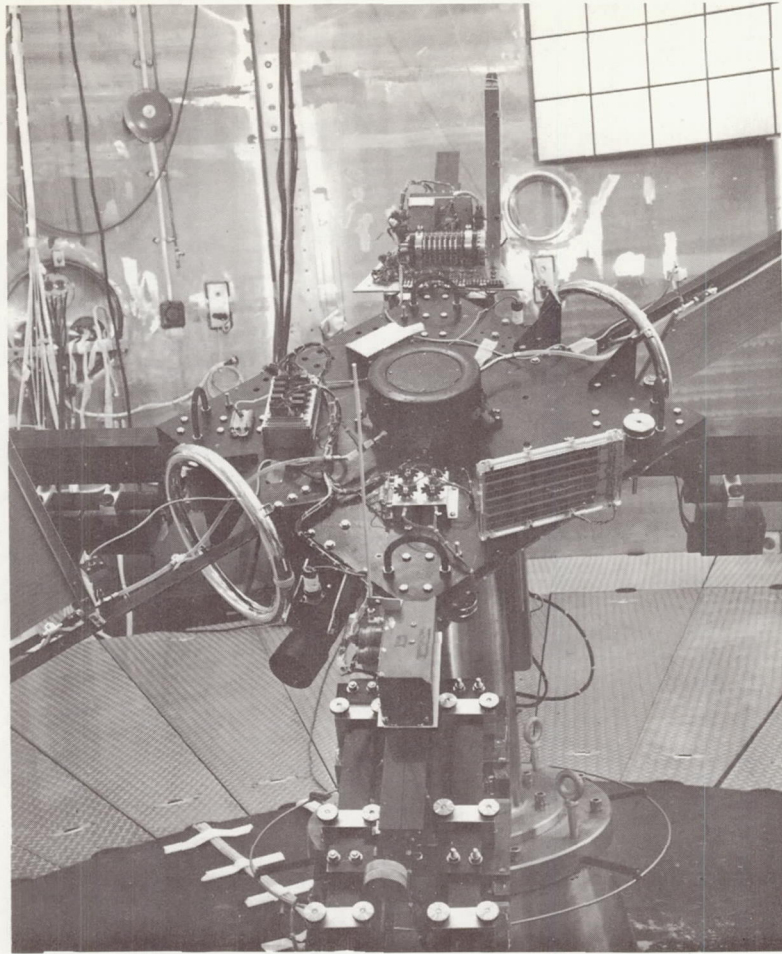- BATTERIES
- RECEIVER
- GAS BEARING PEDESTAL

Figure 10—Gas bearing used in simulation of attitude control system.

to the spin axis and aligned with the center of the ball. The output of the arrays, which were set up 90° apart, locates the spin axis to within 0.1° of its true position in space.

In the region near the local vertical, where most of the testing was conducted, the space is virtually divided into rectangular coordinates, with each array giving an independent coordinate. The basic attitude determination system involved gray code logic and provided serial binary information on a strip chart recorder; automatic position plotting also was incorporated.

In ground testing, motion of the spin axis occurs even in the absence of control torques, because of static and dynamic unbalance, and the rotation of the earth. In practice, the displacement of the center of mass from the spin axis, and also dynamic unbalance, proved to have negligible effects. The "natural drift" tendency of the spin axis was dominated by the displacement of the center of mass along the spin axis, and the rotation of the earth. The result was a precession of the spin axis on a cone the center of which was on a north-south line throughout the ball (Figure 11—see Appendix C for analysis).

If the spin axis is aligned with the local vertical when the table is uncaged, the initial drift will always be to the west. In general, it will then curve north if the table is pendulous, and south if it is top-heavy. The dividing line itself, a due west drift, is a possible path for a slightly top-heavy condition. Physical constraints permitting, the spin axis will move on a cone, eventually returning to a vertical position. The position of the precession axis was very sensitive to the simulator unbalance, which in turn was easily adjustable. Thus the "natural drift" characteristic could be significantly altered by changing the position of the balance weight. This capability was used to bring the spin axis back to the local vertical before caging.
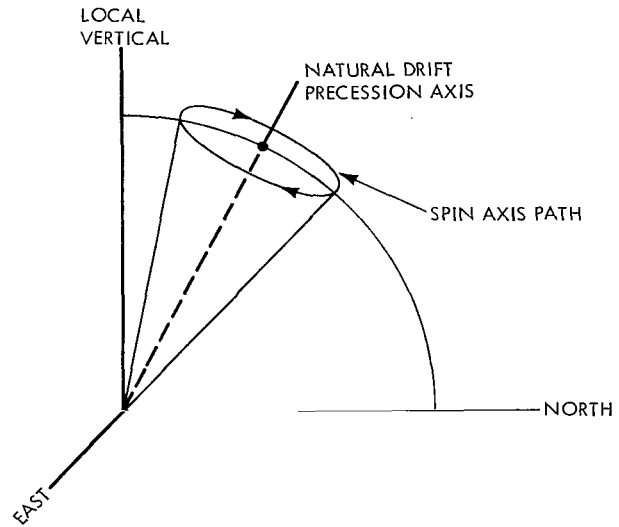

Figure 11—Natural drift of spin axis.

The attitude determination arrays were set up due north and due west of the air bearing table with the "sun pulse" corresponding to the time of illumination of the north array. Thus, in effect, the sun was always north of the table and, with the spin axis in the vicinity of the local vertical, the direction of the several torques produced by the thruster system was due east or due north, etc.

Most testing was performed in a well-balanced condition so that the natural drift tendency was due west and represented a steady-state perturbation which could easily be accounted for. Resultant motion during one execute command for the various modes is illustrated in Figure 12.

Figure 13 shows the experimental precession angle per command (approximately 70 torque pulses in 2.74 minutes) determined for the Freon thruster ACS. These data are based on a detailed
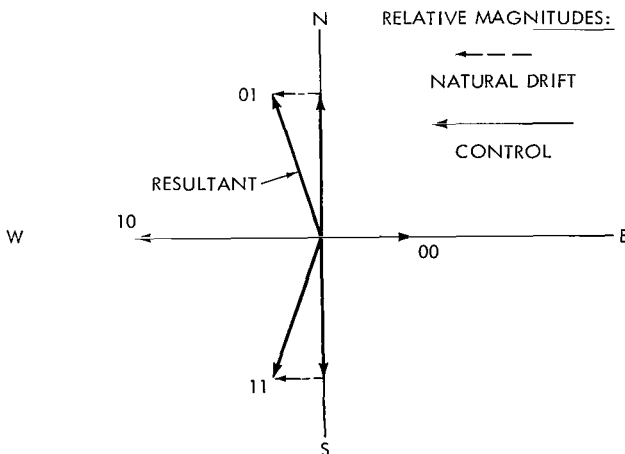

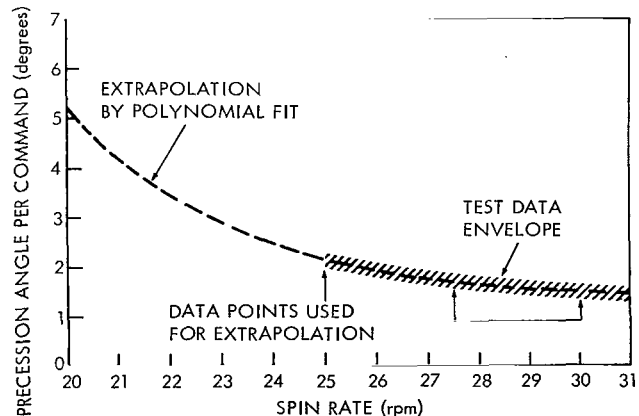Figure 12—Typical spin axis motion.

Figure 13—Predicted performance of cold gas ACS.

analysis of 72 precession commands issued during the gas bearing testing. From the figure, it will be apparent that precession angle at the nominal spin rate of 27.5 rpm is 1.72 ± .06 degrees. Data were gathered for spin rates over the range of 25 to 31 rpm and extrapolated to lower spin rates by a third-degree polynomial fit. During early testing, it was found that the precession directions were in error by about 8 degrees with respect to the desired directions because of a long thrust decay time. This was corrected (pulse shape changed) by increasing the throat diameter of the thruster nozzle prior to the final air bearing test. Appendix D describes a unique method of determining a precession direction from pressure transducer data.

FLIGHT OPERATIONS AND SYSTEM PERFORMANCE

In flight, the attitude control system was used for two purposes:

a. Reorientation of the spin axis prior to 4th stage ignition for refinement of lunar orbit parameters.

b. Establishment of a scientifically preferable attitude, perpendicular to the ecliptic.

The first maneuver involved three commands in the 11 mode (south) to increase the sun aspect angle by 5.55°. Based on the initial maneuver, a precession angle of 1.85 degrees per command was obtained. This is slightly higher performance than anticipated. Also, a specific impulse, I_{sp}, was calculated based on average mass flow and found to be approximately 50 lb-seconds per pound of fuel. Later, the spin axis was moved to the south ecliptic pole with 40 commands in the 10 mode (west) and 16 commands in the 01 mode (north). Figure 14 illustrates these maneuvers. It is of interest to report that the sun angle did not change during the entire out-of-plane (spin axis-sunline plane, 10 mode) maneuver. This verifies the theory, equations, and air bearing tests developed in earlier sections.
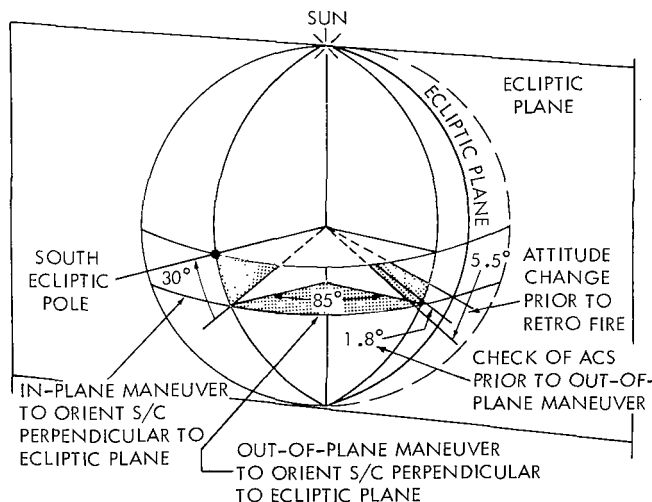
Further, the attitude control system was exercised in January and July 1968 and also January 1969 (6, 12 and 18 months after launch) and its performance remained nominal. These successful operations demonstrated the usefulness of the system after as much as 18 months exposure to the lunar space environment.

Figure 14—Explorer XXXV flight reorientation.

Appendix A

Subliming Solid Thrusters

As was mentioned earlier, subliming solid thrusters, a new technology, were considered for the AIMP E attitude control system. Technical problems as well as the spacecraft flight schedule prevented installation of the thrusters. The following gives a brief description of the thruster system and some of the problems encountered.

The subliming solid thrusters were designed and built by Rocket Research Corporation; Figure A1 shows the system schematic, and Figure A2 shows the assembled unit. The fuel tank is toroidally shaped, with valves, heaters, and filters centrally mounted and enclosed within thermal shields. It was designed to fit into the available space in the center tube of the spacecraft just above the 3rd stage separation plane. The location of the nozzles on deployable solar paddles made flexible (teflon) lines necessary, and manual valves were included for protecting the solenoid valves from air and/or moisture contamination.
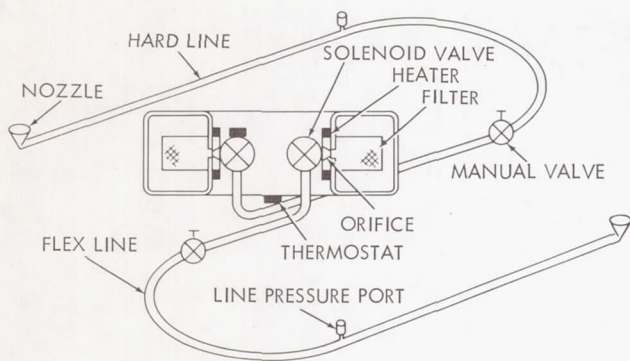

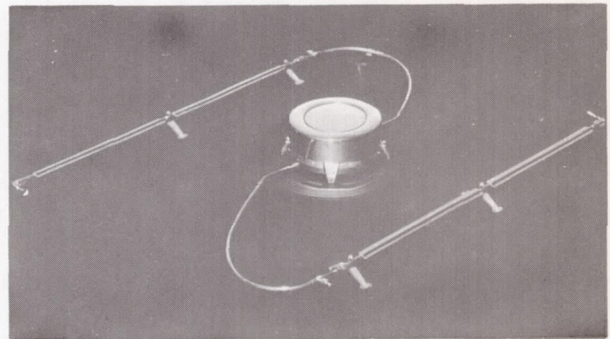Figure A1—Subliming solid thruster schematic.

Figure A2—Subliming solid thruster system.

As might be inferred from the presence of heaters and thermostats, the thermal condition is an important factor in the operating scheme. Besides the need for supplying the heat for sublimation, there is a problem in the fact that recondensation of fuel in certain portions of the system can affect performance. The design objectives were, first, to make the temperature of the solenoid valve/filter area higher than that of any other area of the tank and, second, to provide a positive temperature gradient along the lines from valves to nozzles to prevent fuel recondensation during operation. The system was thus designed to be thermally isolated from the spacecraft, and all radiating surfaces were gold plate for its high α/ϵ ratio.

The ammonium hydrosulfide fuel, also known as ammonium bisulfide (NH_4HS), has a vapor pressure of 7 psia at room temperature (20°C), which increases by about 3.5 psia with every 10°C rise in temperature. It sublimes producing H_2S and NH_3, a toxic and highly corrosive mixture. Another property which presents problems for valve operation is that sulfur and polysulfides which are non-volatile are formed on contact with oxygen. Precautions were therefore taken to limit exposure of the fuel to either vacuum or a high-purity argon atmosphere.

Every malfunction experienced, with the exception of recondensation in the lines during an overtest, is traceable to fuel effects on the valve. There had been but one valve successfully used with the fuel. It could not be considered, because of its high residual magnetic field. The valve selected was especially designed by a valve manufacturer for this application, and also featured a low (1-watt) power consumption. Modifications to the valve while attempting to qualify the system included: increasing power to 2 watts; change of poppet material from tungsten carbide to Kel-F, then to stainless steel; and change of seat material from stainless steel to neoprene. Corrosion and non-volatiles persistently plagued operation by rendering the valve inoperable or leaking. Neoprene presented further difficulties, first with inadequate curing and finally by taking permanent set despite a good cure. Follow-on work with neoprene was also not completely successful, a result which may stem from an incompatibility of one or more of its many (>20) constituents. The formerly successful valve had a teflon seat with a stainless steel poppet which could not readily be incorporated in the AIMP E valve, but it may prove to be the only solution to the valve problem for future NH_4HS systems.

Appendix B

Nutation Damper

1.0 Mechanical Data

Dimensions		See Figure B1

Weights -

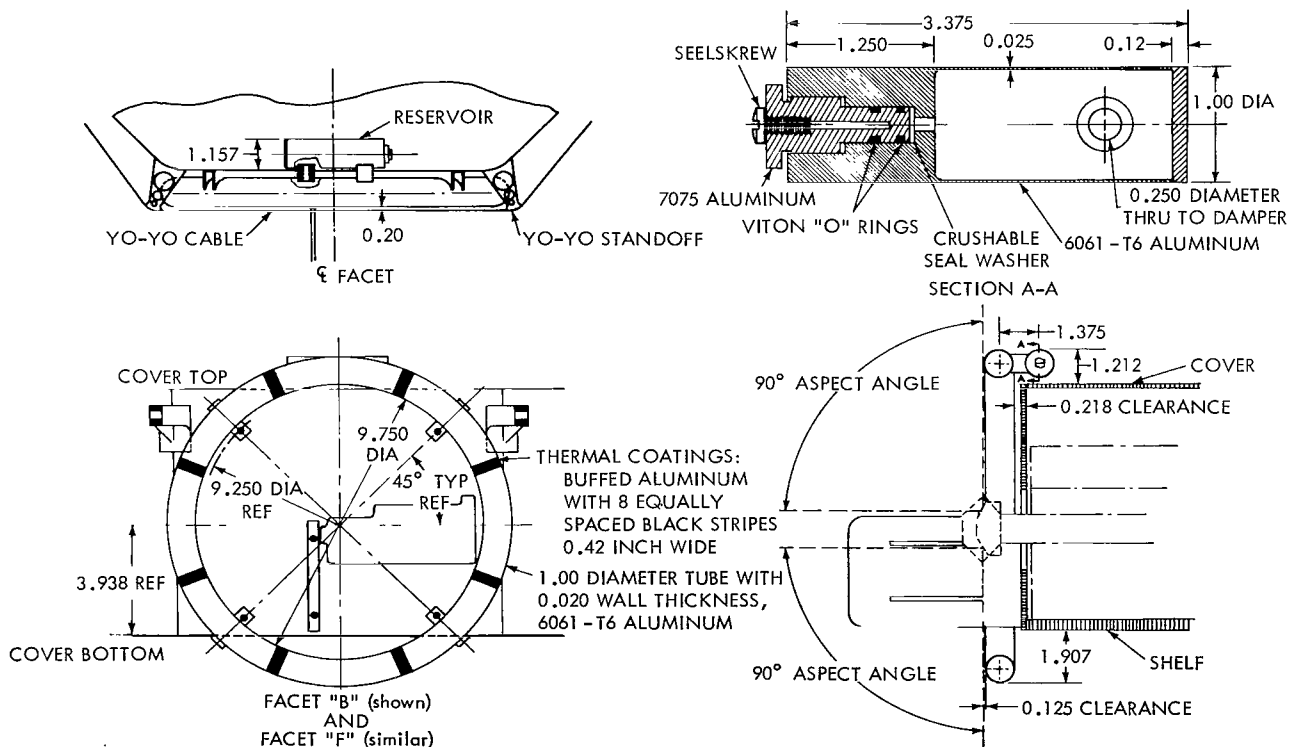|		
1 empty damper assembly		0.41 lb
Fluid charge for 1 damper	·	0.86 lb
Total weight per damper		1.27 lb
Number of dampers per system		2*

Figure B1—Nutation damper.

---

*Only one damper was carried aboard Explorer XXXV.

2.0 Performance Data

Time Constants

Nominal at 25 rpm and 77°F

During transfer trajectory	33.7 minutes
During lunar orbit (post-retro separation)	15.7 minutes
As functions of temperature and spin rates	See Figure B2

Figure B2—Time constants for nutation damper.

Note:

(1) The dampers are tuned to the transfer trajectory inertial characteristics and nominal spin rate.

(2) The following assumptions were made in computing the above time constants:

(a) I_Z = 15.36 slug-ft^2
I_X = 13.68 slug-ft^2 }Transfer trajectory
I_Y = 7.24 slug-ft^2

(b) I_Z = 15.02 slug-ft^2
I_X = 10.93 slug-ft^2 }Orbital mode
I_Y = 4.56 slug-ft^2

(c) Spin rate = 25 rpm

(d) Temperature = 77°F

(e) Ring radius = 0.448 ft

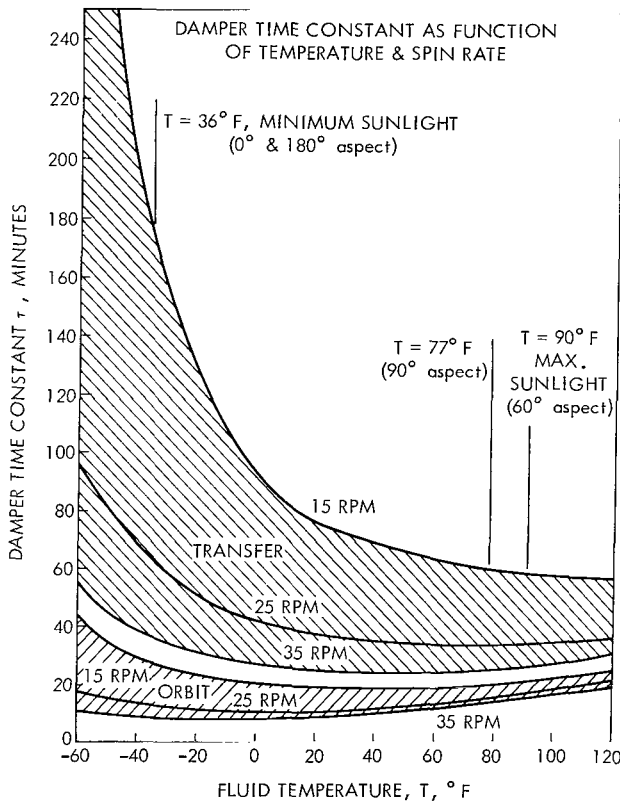(3) Time constant calculations were made using the following equations:

$$\tau = \frac{\epsilon}{2} \frac{C - A}{.19\, mR^2 \frac{nC}{A}} \sqrt{\frac{AB}{(C-B)(C-A)}} \text{ seconds },$$

where A, B, C = inertias (slug-ft^2) in ascending order (A < B < C),

n = spin rate (rad/sec),

m = mass of fluid per damper,

R = ring radius (ft).

Let

$$x = a \sqrt{\frac{100N}{\nu}} ,$$

where

$$N = n \sqrt{\frac{(C-B)(C-A)}{AB}} \ \text{rad/sec} ,$$

ν = viscosity in centistokes,

a = tube radius (inches).

ϵ depends on x as follows:

x	ϵ
.25	6
.5	1.7
1	1
2	1.7
5	4
10	7.5

Appendix C

Natural Drift of Satellite Simulator

Let

$\vec{k}$ = unit vector along the spin axis

$\vec{v}$ = unit vector along the local vertical

M = static unbalance (weight of the simulator × displacement of the center of mass from the center of the ball, measured along the spin axis), positive when pendulous.

The unbalance moment is then

$$\vec{M} = M \vec{k} \times \vec{v}$$

and the equation of motion in a local reference frame is

$$\frac{d}{dt} \vec{H} + \vec{\Omega} \times \vec{H} = M \vec{k} \times \vec{v} \, ,$$

where

$\vec{\Omega}$ = earth's angular velocity vector.

Assuming that $\vec{H} = H \vec{k}$, it can be shown that

H = constant, so the equation becomes

$$\frac{d}{dt} \vec{k} + \vec{\Omega} \times \vec{k} = \frac{M}{H} \vec{k} \times \vec{v} \, ,$$

$$\frac{d}{dt} \vec{k} = \vec{k} \times \left(\frac{M}{H} \vec{v} + \vec{\Omega} \right) \, .$$

The vector in brackets is a constant in the local frame. Dotting both sides by this vector shows that

$$\vec{k} \cdot \left[\frac{M}{H} \vec{v} + \vec{\Omega} \right] = \text{constant} \, ,$$

so that the spin axis must rotate about the vector $(M/H) \vec{v} + \vec{\Omega}$.

19

We can then write the precession vector

$$\omega_p = \dot{\varphi}\, \frac{\frac{M}{H}\vec{v} + \vec{\Omega}}{\left|\frac{M}{H}\vec{v} + \vec{\Omega}\right|}$$

and express

$$\frac{d}{dt}\vec{k} \text{ as } \vec{\omega}_p \times \vec{k} .$$

Then

$$\dot{\varphi}\, \frac{\frac{M}{H}\vec{v} + \vec{\Omega}}{\left|\frac{M}{H}\vec{v} + \vec{\Omega}\right|} \times \vec{k} = \vec{k} \times \left[\frac{M}{H}\vec{v} + \vec{\Omega}\right] ,$$

and

$$\dot{\varphi} = -\left|\frac{M}{H}\vec{v} + \vec{\Omega}\right| .$$

Now Goddard Space Flight Center lies at a latitude of 39°, and the earth rotates once in 23h 56m 04s ($\Omega = 0.000073$ radians per second), so $\vec{\Omega}$ has a vertical component of 0.000046 rad/sec and a northern component of 0.0000565 rad/sec. Thus

$$\dot{\varphi} = -\sqrt{\left(\frac{M}{H} + 0.000046\right)^2 + (0.0000565)^2} .$$

The angle α between the precession axis and the local vertical is given by

$$\tan \alpha = \frac{0.0000565}{\frac{M}{H} + 0.000046} .$$

Figure C1 shows a summary of these results.

α and $\dot{\varphi}$ are each observable, and either can provide an accurate measure of the unbalance M. Final balance is best achieved by determining M in this way (by observing the natural drift) and then moving an adjustable weight to compensate for it.
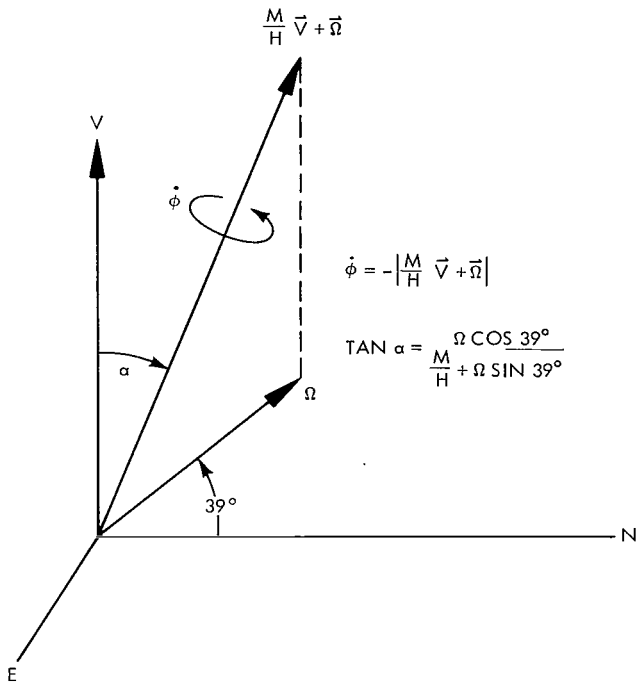
20

$$\frac{M}{H}\vec{V} + \vec{\Omega}$$

$$\dot{\phi} = -\left|\frac{M}{H}\vec{V} + \vec{\Omega}\right|$$

$$\tan \alpha = \frac{\Omega \cos 39°}{\frac{M}{H} + \Omega \sin 39°}$$

Figure C1—Natural drift of spin axis of
satellite simulator.

Precession period and α as functions of M/H are shown in Table C1. With good balance and with the spin axis nearly vertical, the spin axis will tip to the west at a rate of about 0.2 degrees per minute.

Table C1

Natural Drift Precession Period and Angle α.

M/H	Precession Period	Angle α
.012514	8.3 min	0.25°
.006234	16.6 min	0.50°
.003094	33.3 min	1°
.001569	1.08 hr	2°
.000596	2.7 hr	5°
.000275	5.35 hr	10°
.0001092	10.56 hr	20°
.0000519	15.42 hr	30°
.0000213	19.87 hr	40°
.0000014	23.6 hr	50°
−.0000134	26.7 hr	60°
−.0000254	29.0 hr	70°
−.0000360	30.4 hr	80°
−.0000460	30.9 hr	90°
−.0000560	30.4 hr	100°
−.0000666	29.0 hr	110°
−.0000786	26.7 hr	120°
−.0000934	23.6 hr	130°
−.0001133	19.87 hr	140°
−.0001439	15.42 hr	150°
−.0002012	10.56 hr	160°
−.0003670	5.35 hr	170°
−.0006880	2.7 hr	175°
−.001661	1.08 hr	178°
−.003186	33.3 min	179°
−.006326	16.6 min	179.5°
−.012606	8.3 min	179.75°

Appendix D

Determination of Precession Direction from Pressure Transducer Data

Consider an attitude control system, for a spinning spacecraft, which provides a torque perpendicular to the spin axis during a portion of a rotation period. Let the torque be provided by a pair of thrusters at some distance from a gas supply and valves, with the static pressure in the connecting lines monitored. Assume that the thrust developed is proportional to the measured line pressure.

Let the torque levels be small enough that the momentum change during one revolution of the spacecraft takes place in a plane perpendicular to the initial spin vector. Figure D1 shows the torque vector at some time t referred to an arbitrary line in this plane.

Since

$$\frac{d}{dt} \vec{H} = \vec{T} ,$$

we can say, for a single pulse,

$$(\Delta H)_x = \int T(t) \cos \theta(t) \, dt$$

and

$$(\Delta H)_y = \int T(t) \sin \theta(t) \, dt ,$$

where the integration is performed over the entire pulse width. ΔH will then be the square root of the sum of the squares of $(\Delta H)_x$ and $(\Delta H)_y$, and the direction of ΔH can be expressed as (see Figure D2).

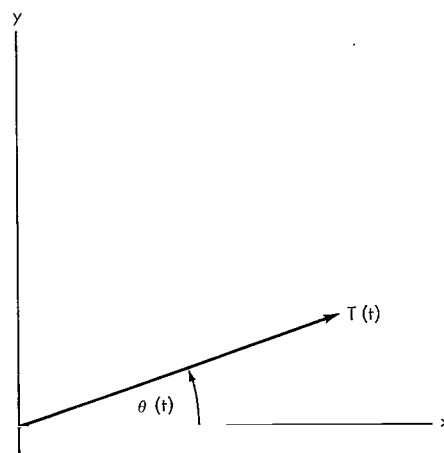$$\tan \phi = \frac{(\Delta H)_y}{(\Delta H)_x} = \frac{\int T(t) \sin \theta(t) \, dt}{\int T(t) \cos \theta(t) \, dt} .$$

Figure D1—Torque vector.

23

Figure D2—Directional angle.

Figure D3—Centroid of polar plot of $\sqrt[3]{p}$ (θ).

For a constant spin rate, θ increases uniformly and may be substituted as the independent variable, then
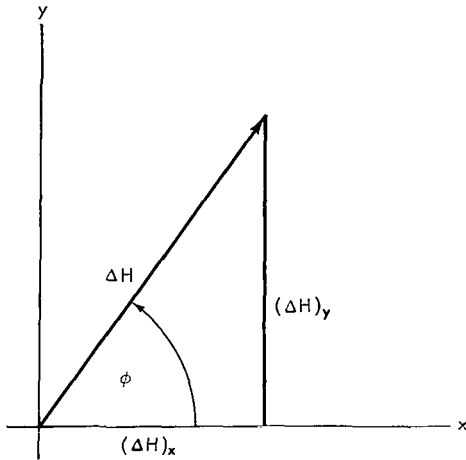
$$\tan \phi = \frac{\int T(\theta) \sin \theta \, d\theta}{\int T(\theta) \cos \theta \, d\theta}$$

$$= \frac{\int p(\theta) \sin \theta \, d\theta}{\int p(\theta) \cos \theta \, d\theta}$$

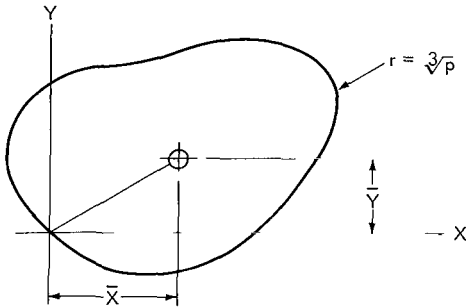if $T \propto p$, where p is the line pressure.

Now consider a plot of $\sqrt[3]{p}$ (θ) in polar coordinates, and in particular the direction of the line joining the origin to the centroid of the resulting area (Figure D3):

In polar coordinates $dA = r \, dr \, d\theta$, $x = r \cos \theta$, $y = r \sin \theta$, so

$$\bar{y} = \frac{\iint y \, dA}{A}, \qquad \bar{x} = \frac{\iint x \, dA}{A}$$

$$\frac{\bar{y}}{\bar{x}} = \frac{\iint y \, dA}{\iint x \, dA} = \frac{\int d\theta \int_0^{\sqrt[3]{p}} dr \left(r^2 \sin \theta\right)}{\int d\theta \int_0^{\sqrt[3]{p}} dr \left(r^2 \cos \theta\right)}$$

$$= \frac{\int p(\theta) \sin \theta \, d\theta}{\int p(\theta) \cos \theta \, d\theta}$$

$$= \tan \phi \ .$$

Thus the location of the centroid of a polar plot of $\sqrt[3]{p}(\theta)$ reveals the direction in which a move takes place with a given pressure pulse.

"The aeronautical and space activities of the United States shall be conducted so as to contribute . . . to the expansion of human knowledge of phenomena in the atmosphere and space. The Administration shall provide for the widest practicable and appropriate dissemination of information concerning its activities and the results thereof."

— NATIONAL AERONAUTICS AND SPACE ACT OF 1958

NASA SCIENTIFIC AND TECHNICAL PUBLICATIONS

TECHNICAL REPORTS: Scientific and technical information considered important, complete, and a lasting contribution to existing knowledge.

TECHNICAL NOTES: Information less broad in scope but nevertheless of importance as a contribution to existing knowledge.

TECHNICAL MEMORANDUMS: Information receiving limited distribution because of preliminary data, security classification, or other reasons.

CONTRACTOR REPORTS: Scientific and technical information generated under a NASA contract or grant and considered an important contribution to existing knowledge.

TECHNICAL TRANSLATIONS: Information published in a foreign language considered to merit NASA distribution in English.

SPECIAL PUBLICATIONS: Information derived from or of value to NASA activities. Publications include conference proceedings, monographs, data compilations, handbooks, sourcebooks, and special bibliographies.

TECHNOLOGY UTILIZATION PUBLICATIONS: Information on technology used by NASA that may be of particular interest in commercial and other non-aerospace applications. Publications include Tech Briefs, Technology Utilization Reports and Notes, and Technology Surveys.

Details on the availability of these publications may be obtained from:

SCIENTIFIC AND TECHNICAL INFORMATION DIVISION

NATIONAL AERONAUTICS AND SPACE ADMINISTRATION

Washington, D.C. 20546